

# 1 Supplementary material for LHCb-PAPER-2019-028

This appendix contains supplementary material that will be posted on the public CDS record but will not appear in the paper.

The definition of the binning scheme  $B$  is reported in Table 1. In addition, the contribution of each candidate to the energy test result is presented for the  $P$ -even test for  $CP$ -violation in Fig. 1, for the distance scale  $\delta = 2.7\text{GeV}^2/c^4$ . This uses the method set out in Ref. [1], whereby the contribution from each candidate  $i$  to the overall test statistic  $T$  is quantified by a value  $T_i$  and then the ‘significance’ of this contribution is considered.

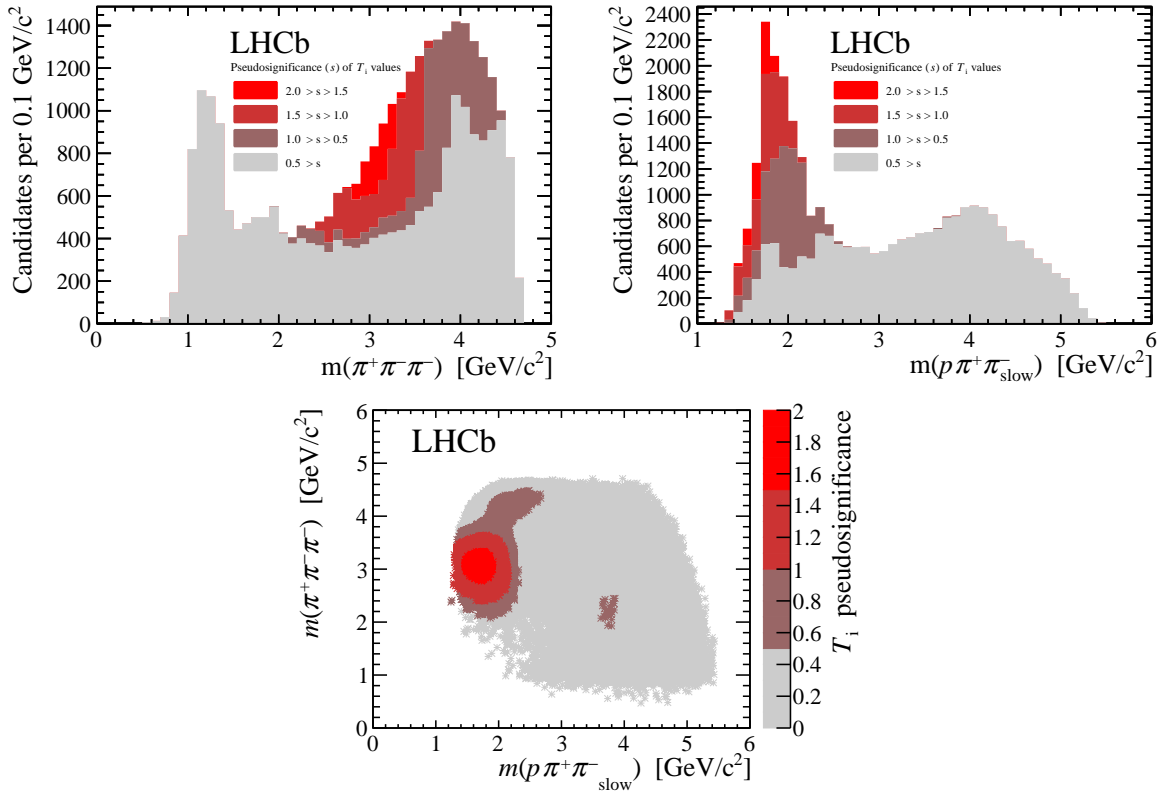


Figure 1: Candidates are classed by their relative contribution to the overall value of  $T$ . The distributions of these different classes are then displayed as a function of different invariant masses formed from combining the final-state particles.

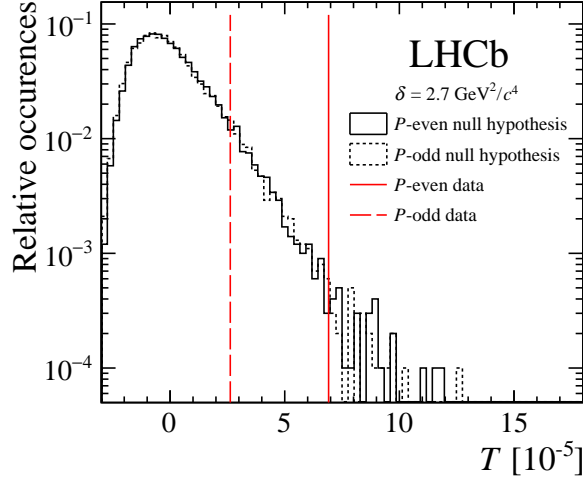


Figure 2: Distributions of  $T$  under the null hypothesis obtained from permutations, using the energy test with  $\delta = 2.7 \text{ GeV}^2/c^4$  in the  $P$ -even and  $P$ -odd configurations when searching for  $CP$  violation. The values of  $T$  obtained from data are shown as vertical lines.

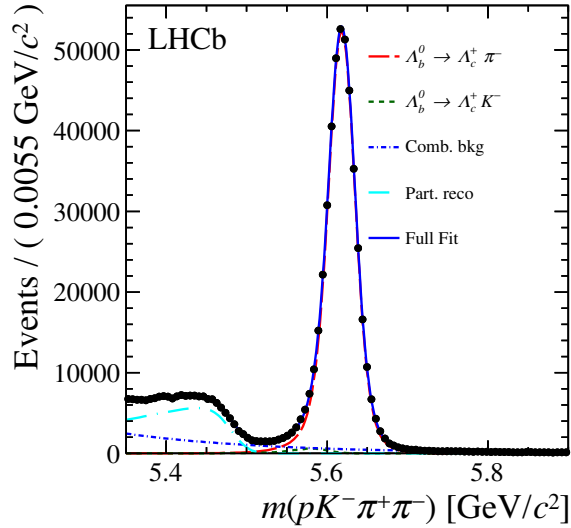


Figure 3: Invariant mass distribution for  $\Lambda_b^0 \rightarrow \Lambda_c^+ (\rightarrow pK^- \pi^+) \pi^-$  candidates with the result of the fit overlaid. The solid and dotted lines describe the projections of the fit results for various components as listed in the legend.

Table 1: Definition of binning scheme  $B$ . This binning scheme is based on the helicity angles of the decay topology  $\Lambda_b^0 \rightarrow (N^{*+} \rightarrow (\Delta^{++} \rightarrow p\pi^+) \pi^-) \pi^-$  where  $\varphi$  is the azimuthal angle of the proton in the  $\Delta^{++}$  rest frame and  $\theta_{\Delta^{++}}$  ( $\theta_p$ ) is the polar angle of the  $\Delta^{++}$  ( $p$ ) in the  $N^{*+}$  ( $\Delta^{++}$ ) rest frame.

Bin number	Polar angles	Azimuthal angles
1	$\theta_p \in [0, \pi/4]$ and $\theta_{\Delta^{++}} \in [0, \pi/4]$ $\theta_p \in [\pi/2, 3\pi/4]$ and $\theta_{\Delta^{++}} \in [\pi/2, 3\pi/4]$	$ \varphi  \in [0, \pi/2]$
2	$\theta_p \in [0, \pi/4]$ and $\theta_{\Delta^{++}} \in [\pi/4, \pi/2]$ $\theta_p \in [\pi/2, 3\pi/4]$ and $\theta_{\Delta^{++}} \in [3\pi/4, \pi]$	$ \varphi  \in [0, \pi/2]$
3	$\theta_p \in [0, \pi/4]$ and $\theta_{\Delta^{++}} \in [\pi/2, 3\pi/4]$ $\theta_p \in [\pi/2, 3\pi/4]$ and $\theta_{\Delta^{++}} \in [0, \pi/4]$	$ \varphi  \in [0, \pi/2]$
4	$\theta_p \in [0, \pi/4]$ and $\theta_{\Delta^{++}} \in [3\pi/4, \pi]$ $\theta_p \in [\pi/2, 3\pi/4]$ and $\theta_{\Delta^{++}} \in [\pi/4, \pi/2]$	$ \varphi  \in [0, \pi/2]$
5	$\theta_p \in [\pi/4, \pi/2]$ and $\theta_{\Delta^{++}} \in [0, \pi/4]$ $\theta_p \in [3\pi/4, \pi]$ and $\theta_{\Delta^{++}} \in [\pi/2, 3\pi/4]$	$ \varphi  \in [0, \pi/2]$
6	$\theta_p \in [\pi/4, \pi/2]$ and $\theta_{\Delta^{++}} \in [\pi/4, \pi/2]$ $\theta_p \in [3\pi/4, \pi]$ and $\theta_{\Delta^{++}} \in [3\pi/4, \pi]$	$ \varphi  \in [0, \pi/2]$
7	$\theta_p \in [\pi/4, \pi/2]$ and $\theta_{\Delta^{++}} \in [\pi/2, 3\pi/4]$ $\theta_p \in [3\pi/4, \pi]$ and $\theta_{\Delta^{++}} \in [0, \pi/4]$	$ \varphi  \in [0, \pi/2]$
8	$\theta_p \in [\pi/4, \pi/2]$ and $\theta_{\Delta^{++}} \in [3\pi/4, \pi]$ $\theta_p \in [3\pi/4, \pi]$ and $\theta_{\Delta^{++}} \in [\pi/4, \pi/2]$	$ \varphi  \in [0, \pi/2]$
9	$\theta_p \in [0, \pi/4]$ and $\theta_{\Delta^{++}} \in [0, \pi/4]$ $\theta_p \in [\pi/2, 3\pi/4]$ and $\theta_{\Delta^{++}} \in [\pi/2, 3\pi/4]$	$ \varphi  \in [\pi/2, \pi]$
10	$\theta_p \in [0, \pi/4]$ and $\theta_{\Delta^{++}} \in [\pi/4, \pi/2]$ $\theta_p \in [\pi/2, 3\pi/4]$ and $\theta_{\Delta^{++}} \in [3\pi/4, \pi]$	$ \varphi  \in [\pi/2, \pi]$
11	$\theta_p \in [0, \pi/4]$ and $\theta_{\Delta^{++}} \in [\pi/2, 3\pi/4]$ $\theta_p \in [\pi/2, 3\pi/4]$ and $\theta_{\Delta^{++}} \in [0, \pi/4]$	$ \varphi  \in [\pi/2, \pi]$
12	$\theta_p \in [0, \pi/4]$ and $\theta_{\Delta^{++}} \in [3\pi/4, \pi]$ $\theta_p \in [\pi/2, 3\pi/4]$ and $\theta_{\Delta^{++}} \in [\pi/4, \pi/2]$	$ \varphi  \in [\pi/2, \pi]$
13	$\theta_p \in [\pi/4, \pi/2]$ and $\theta_{\Delta^{++}} \in [0, \pi/4]$ $\theta_p \in [3\pi/4, \pi]$ and $\theta_{\Delta^{++}} \in [\pi/2, 3\pi/4]$	$ \varphi  \in [\pi/2, \pi]$
14	$\theta_p \in [\pi/4, \pi/2]$ and $\theta_{\Delta^{++}} \in [\pi/4, \pi/2]$ $\theta_p \in [3\pi/4, \pi]$ and $\theta_{\Delta^{++}} \in [3\pi/4, \pi]$	$ \varphi  \in [\pi/2, \pi]$
15	$\theta_p \in [\pi/4, \pi/2]$ and $\theta_{\Delta^{++}} \in [\pi/2, 3\pi/4]$ $\theta_p \in [3\pi/4, \pi]$ and $\theta_{\Delta^{++}} \in [0, \pi/4]$	$ \varphi  \in [\pi/2, \pi]$
16	$\theta_p \in [\pi/4, \pi/2]$ and $\theta_{\Delta^{++}} \in [3\pi/4, \pi]$ $\theta_p \in [3\pi/4, \pi]$ and $\theta_{\Delta^{++}} \in [\pi/4, \pi/2]$	$ \varphi  \in [\pi/2, \pi]$

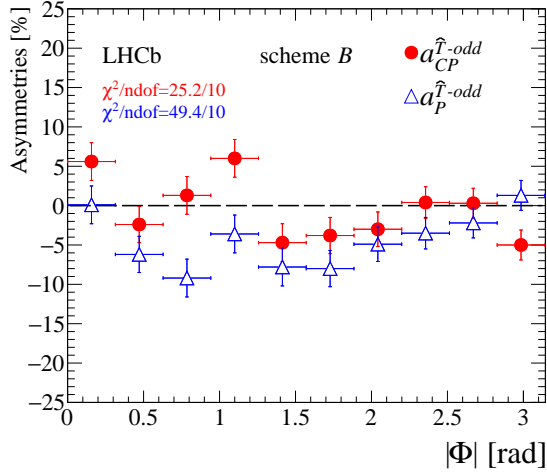


Figure 4: Measured asymmetries for binning scheme  $B$ . The error bars represent the sum in quadrature of the statistical and systematic uncertainties. The  $\chi^2/\text{ndof}$  is calculated with respect to the null hypothesis and it includes statistical and systematic uncertainties.

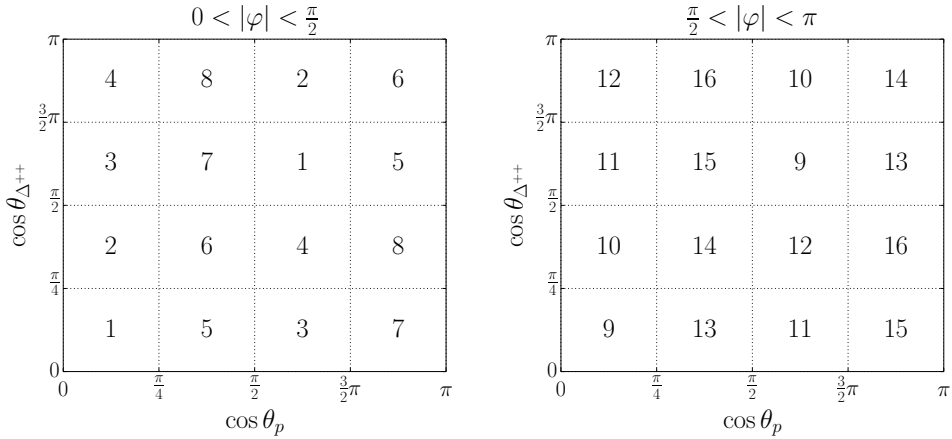


Figure 5: Graphical visualisation of the binning scheme definition for scheme  $A$ .

Table 2: Results obtained with different binning schemes; the  $p$ -values take into account systematic effects and are reported for the  $CP$ - and  $P$ -conserving hypotheses.

Binning scheme	Dominant contribution	Hypothesis	$p$ -value
$A_1$ (helicity angles)	$\Lambda_b^0 \rightarrow pa_1^-$	$CP$ -conserving	$9.8 \times 10^{-2}$
		$P$ -conserving	$1.8 \times 10^{-5}$
$A_2$ (helicity angles)	$\Lambda_b^0 \rightarrow N^{*+}\pi^-$	$CP$ -conserving	$6.4 \times 10^{-1}$
		$P$ -conserving	$6.4 \times 10^{-2}$
$B$ (in $ \Phi $ )	Entire sample	$CP$ -conserving	$5.0 \times 10^{-3}$
		$P$ -conserving	$3.5 \times 10^{-7}$
$B_1$ (in $ \Phi $ )	$\Lambda_b^0 \rightarrow pa_1^-$	$CP$ -conserving	$4.7 \times 10^{-2}$
		$P$ -conserving	$4.3 \times 10^{-8}$
$B_2$ (in $ \Phi $ )	$\Lambda_b^0 \rightarrow N^{*+}\pi^-$	$CP$ -conserving	$3.4 \times 10^{-3}$
		$P$ -conserving	$1.9 \times 10^{-3}$

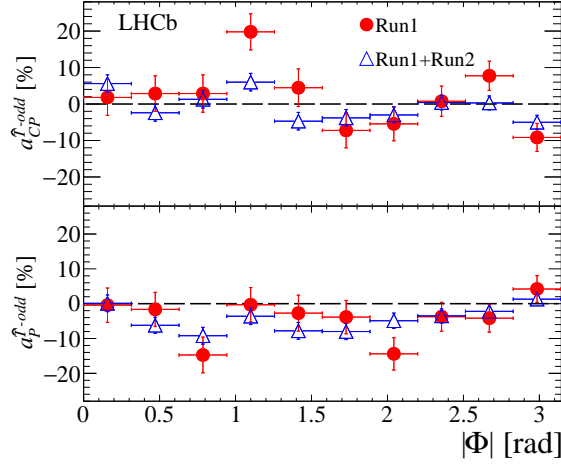


Figure 6: Measured asymmetries for binning scheme  $B$  with different datasets. The error bars represent the sum in quadrature of the statistical and systematic uncertainties.

Table 3: Measured asymmetries in bins of the helicity angles in the region of the phase space dominated by the  $A_b^0 \rightarrow pa_1$  contribution (scheme  $A_1$ ). The first (second) error represents the statistic (systematic) uncertainty.

Bin	$A_{\hat{T}}(\%)$	$\bar{A}_{\hat{T}}(\%)$	$a_{\hat{T}}^{\text{odd}}(\%)$	$a_{CP}^{\hat{T}\text{-odd}}(\%)$
1	$-8.2 \pm 4.6 \pm 0.8$	$-2.3 \pm 4.5 \pm 0.8$	$-5.2 \pm 3.2 \pm 0.6$	$-3.0 \pm 3.2 \pm 0.6$
2	$-9.4 \pm 2.7 \pm 0.9$	$-4.7 \pm 2.7 \pm 0.9$	$-7.0 \pm 1.9 \pm 0.6$	$-2.3 \pm 1.9 \pm 0.6$
3	$-6.9 \pm 9.0 \pm 1.1$	$-8.5 \pm 8.8 \pm 1.1$	$-7.7 \pm 6.3 \pm 0.8$	$0.8 \pm 6.3 \pm 0.8$
4	$-5.9 \pm 5.4 \pm 1.7$	$2.7 \pm 5.4 \pm 1.7$	$-1.6 \pm 3.8 \pm 1.2$	$-4.3 \pm 3.8 \pm 1.2$
5	$-38.8 \pm 11.4 \pm 2.2$	$8.2 \pm 9.9 \pm 2.2$	$-15.3 \pm 7.6 \pm 1.6$	$-23.5 \pm 7.6 \pm 1.6$
6	$-26.6 \pm 8.9 \pm 2.6$	$-22.3 \pm 9.5 \pm 2.6$	$-24.4 \pm 6.6 \pm 1.8$	$-2.2 \pm 6.6 \pm 1.8$
7	$-12.6 \pm 9.2 \pm 1.1$	$11.4 \pm 9.2 \pm 1.1$	$-0.6 \pm 6.6 \pm 0.8$	$-12.0 \pm 6.6 \pm 0.8$
8	$-4.9 \pm 7.1 \pm 0.9$	$4.4 \pm 8.0 \pm 0.9$	$-0.3 \pm 5.4 \pm 0.6$	$-4.7 \pm 5.4 \pm 0.6$
9	$-15.6 \pm 7.6 \pm 0.6$	$-5.7 \pm 9.2 \pm 0.6$	$-10.7 \pm 6.0 \pm 0.4$	$-4.9 \pm 6.0 \pm 0.4$
10	$-1.4 \pm 4.1 \pm 0.7$	$-11.1 \pm 4.0 \pm 0.7$	$-6.3 \pm 2.9 \pm 0.5$	$4.9 \pm 2.9 \pm 0.5$
11	$-15.2 \pm 7.9 \pm 1.2$	$-12.2 \pm 9.1 \pm 1.2$	$-13.7 \pm 6.0 \pm 0.9$	$-1.5 \pm 6.1 \pm 0.9$
12	$4.6 \pm 4.2 \pm 1.1$	$-2.5 \pm 4.2 \pm 1.1$	$1.0 \pm 3.0 \pm 0.8$	$3.6 \pm 3.0 \pm 0.8$
13	$-10.2 \pm 8.5 \pm 0.9$	$-2.6 \pm 8.4 \pm 0.9$	$-6.4 \pm 6.0 \pm 0.7$	$-3.8 \pm 6.0 \pm 0.7$
14	$-6.7 \pm 8.3 \pm 1.2$	$-12.6 \pm 8.2 \pm 1.2$	$-9.6 \pm 5.8 \pm 0.8$	$3.0 \pm 5.9 \pm 0.8$
15	$-7.1 \pm 11.2 \pm 0.6$	$10.9 \pm 10.9 \pm 0.6$	$1.9 \pm 7.9 \pm 0.4$	$-9.0 \pm 7.9 \pm 0.4$
16	$-3.9 \pm 14.1 \pm 0.7$	$-10.8 \pm 14.1 \pm 0.7$	$-7.4 \pm 10.1 \pm 0.5$	$3.4 \pm 10.1 \pm 0.5$

Table 4: Measured asymmetries in bins of the helicity angles in the region of the phase space dominated by the  $\Lambda_b^0 \rightarrow N^{*+} \pi^-$  contribution (scheme  $A_2$ ). The first (second) error represents the statistic (systematic) uncertainty.

Bin	$A_{\hat{T}}(\%)$	$\bar{A}_{\hat{T}}(\%)$	$a_P^{\hat{T}\text{-odd}}(\%)$	$a_{CP}^{\hat{T}\text{-odd}}(\%)$
1	$-5.7 \pm 4.1 \pm 0.8$	$-10.0 \pm 4.2 \pm 0.8$	$-7.8 \pm 3.0 \pm 0.6$	$2.2 \pm 3.0 \pm 0.6$
2	$-10.3 \pm 5.8 \pm 0.9$	$6.1 \pm 6.2 \pm 0.9$	$-2.1 \pm 4.2 \pm 0.6$	$-8.2 \pm 4.2 \pm 0.6$
3	$-1.1 \pm 5.7 \pm 1.1$	$-9.7 \pm 5.9 \pm 1.1$	$-5.4 \pm 4.1 \pm 0.8$	$4.3 \pm 4.1 \pm 0.8$
4	$-19.1 \pm 7.7 \pm 1.7$	$-10.0 \pm 7.4 \pm 1.7$	$-14.5 \pm 5.4 \pm 1.2$	$-4.5 \pm 5.4 \pm 1.2$
5	$0.8 \pm 5.2 \pm 2.2$	$-4.2 \pm 5.1 \pm 2.2$	$-1.7 \pm 3.6 \pm 1.6$	$2.5 \pm 3.6 \pm 1.6$
6	$-4.6 \pm 5.3 \pm 2.6$	$-1.2 \pm 5.3 \pm 2.6$	$-2.9 \pm 3.8 \pm 1.8$	$-1.7 \pm 3.8 \pm 1.8$
7	$-2.4 \pm 4.1 \pm 1.1$	$-4.0 \pm 4.0 \pm 1.1$	$-3.2 \pm 2.9 \pm 0.8$	$0.8 \pm 2.9 \pm 0.8$
8	$2.0 \pm 5.4 \pm 0.9$	$-10.3 \pm 5.3 \pm 0.9$	$-4.2 \pm 3.8 \pm 0.6$	$6.2 \pm 3.8 \pm 0.6$
9	$-1.5 \pm 5.1 \pm 0.6$	$-6.7 \pm 4.9 \pm 0.6$	$-4.1 \pm 3.5 \pm 0.4$	$2.6 \pm 3.6 \pm 0.4$
10	$-9.1 \pm 7.4 \pm 0.7$	$1.9 \pm 7.1 \pm 0.7$	$-3.6 \pm 5.2 \pm 0.5$	$-5.5 \pm 5.2 \pm 0.5$
11	$-2.0 \pm 4.7 \pm 1.2$	$3.1 \pm 4.5 \pm 1.2$	$0.6 \pm 3.2 \pm 0.9$	$-2.6 \pm 3.2 \pm 0.9$
12	$-0.4 \pm 7.0 \pm 1.1$	$6.6 \pm 6.6 \pm 1.1$	$3.1 \pm 4.8 \pm 0.8$	$-3.5 \pm 4.9 \pm 0.8$
13	$1.9 \pm 4.1 \pm 0.9$	$-5.2 \pm 4.2 \pm 0.9$	$-1.7 \pm 3.0 \pm 0.7$	$3.5 \pm 3.0 \pm 0.7$
14	$-1.1 \pm 5.7 \pm 1.2$	$-0.3 \pm 5.3 \pm 1.2$	$-0.7 \pm 3.9 \pm 0.8$	$-0.4 \pm 3.9 \pm 0.8$
15	$0.2 \pm 5.0 \pm 0.6$	$3.1 \pm 4.9 \pm 0.6$	$1.7 \pm 3.5 \pm 0.4$	$-1.4 \pm 3.5 \pm 0.4$
16	$8.9 \pm 5.7 \pm 0.7$	$6.6 \pm 5.3 \pm 0.7$	$7.7 \pm 3.9 \pm 0.5$	$1.1 \pm 3.9 \pm 0.5$

Table 5: Measured asymmetries in bins of the  $|\Phi|$  angle (scheme  $B$ ). The first (second) error represents the statistic (systematic) uncertainty.

Bin	$A_{\hat{T}}(\%)$	$\bar{A}_{\hat{T}}(\%)$	$a_P^{\hat{T}\text{-odd}}(\%)$	$a_{CP}^{\hat{T}\text{-odd}}(\%)$
1	$5.7 \pm 3.4 \pm 1.3$	$-5.5 \pm 3.3 \pm 1.3$	$0.1 \pm 2.4 \pm 0.9$	$5.6 \pm 2.4 \pm 0.9$
2	$-8.6 \pm 3.2 \pm 1.2$	$-3.8 \pm 3.4 \pm 1.2$	$-6.2 \pm 2.3 \pm 0.9$	$-2.4 \pm 2.3 \pm 0.9$
3	$-7.8 \pm 3.4 \pm 1.2$	$-10.5 \pm 3.4 \pm 1.2$	$-9.2 \pm 2.4 \pm 0.8$	$1.3 \pm 2.4 \pm 0.8$
4	$2.4 \pm 3.5 \pm 1.1$	$-9.6 \pm 3.4 \pm 1.1$	$-3.6 \pm 2.4 \pm 0.8$	$6.0 \pm 2.4 \pm 0.8$
5	$-12.6 \pm 3.5 \pm 1.1$	$-3.1 \pm 3.3 \pm 1.1$	$-7.8 \pm 2.4 \pm 0.8$	$-4.7 \pm 2.4 \pm 0.8$
6	$-11.8 \pm 3.3 \pm 1.1$	$-4.3 \pm 3.3 \pm 1.1$	$-8.0 \pm 2.3 \pm 0.8$	$-3.8 \pm 2.3 \pm 0.8$
7	$-7.9 \pm 3.1 \pm 1.2$	$-1.8 \pm 3.2 \pm 1.2$	$-4.9 \pm 2.2 \pm 0.8$	$-3.0 \pm 2.2 \pm 0.8$
8	$-3.1 \pm 2.9 \pm 1.1$	$-3.9 \pm 2.9 \pm 1.1$	$-3.5 \pm 2.0 \pm 0.8$	$0.4 \pm 2.0 \pm 0.8$
9	$-1.9 \pm 2.7 \pm 1.0$	$-2.4 \pm 2.7 \pm 1.0$	$-2.2 \pm 1.9 \pm 0.7$	$0.3 \pm 1.9 \pm 0.7$
10	$-3.7 \pm 2.6 \pm 1.0$	$6.3 \pm 2.6 \pm 1.0$	$1.3 \pm 1.9 \pm 0.7$	$-5.0 \pm 1.9 \pm 0.7$

Table 6: Measured asymmetries in bins of the  $|\Phi|$  angle in the region of the phase space dominated by the  $A_b^0 \rightarrow pa_1$  contribution (scheme  $B_1$ ). The first (second) error represents the statistic (systematic) uncertainty.

Bin	$A_{\hat{T}}(\%)$	$\bar{A}_{\hat{T}}(\%)$	$a_{\hat{P}}^{\hat{T}\text{-odd}}(\%)$	$a_{\hat{CP}}^{\hat{T}\text{-odd}}(\%)$
1	$1.6 \pm 4.4 \pm 1.3$	$-10.1 \pm 4.2 \pm 1.3$	$-4.3 \pm 3.0 \pm 0.9$	$5.9 \pm 3.0 \pm 0.9$
2	$-6.9 \pm 4.2 \pm 1.2$	$2.4 \pm 4.5 \pm 1.2$	$-2.3 \pm 3.1 \pm 0.9$	$-4.7 \pm 3.1 \pm 0.9$
3	$-10.2 \pm 4.7 \pm 1.2$	$-12.2 \pm 4.8 \pm 1.2$	$-11.2 \pm 3.4 \pm 0.8$	$1.0 \pm 3.4 \pm 0.8$
4	$-0.2 \pm 5.2 \pm 1.1$	$-2.4 \pm 4.8 \pm 1.1$	$-1.3 \pm 3.5 \pm 0.8$	$1.1 \pm 3.5 \pm 0.8$
5	$-15.6 \pm 5.2 \pm 1.1$	$-5.9 \pm 4.7 \pm 1.1$	$-10.7 \pm 3.5 \pm 0.8$	$-4.9 \pm 3.5 \pm 0.8$
6	$-10.4 \pm 5.0 \pm 1.1$	$-10.3 \pm 5.0 \pm 1.1$	$-10.3 \pm 3.5 \pm 0.8$	$-0.1 \pm 3.5 \pm 0.8$
7	$-10.9 \pm 5.0 \pm 1.2$	$-11.3 \pm 5.5 \pm 1.2$	$-11.1 \pm 3.7 \pm 0.8$	$0.2 \pm 3.7 \pm 0.8$
8	$-12.6 \pm 4.5 \pm 1.1$	$-6.4 \pm 4.7 \pm 1.1$	$-9.5 \pm 3.2 \pm 0.8$	$-3.1 \pm 3.3 \pm 0.8$
9	$-10.8 \pm 4.6 \pm 1.0$	$-3.5 \pm 4.6 \pm 1.0$	$-7.1 \pm 3.2 \pm 0.7$	$-3.7 \pm 3.2 \pm 0.7$
10	$-3.9 \pm 4.4 \pm 1.0$	$15.3 \pm 4.5 \pm 1.0$	$5.7 \pm 3.1 \pm 0.7$	$-9.6 \pm 3.1 \pm 0.7$

Table 7: Measured asymmetries in bins of the  $|\Phi|$  angle in the region of the phase space dominated by the  $A_b^0 \rightarrow N^{*+}\pi^-$  contribution (scheme  $B_2$ ). The first (second) error represents the statistic (systematic) uncertainty.

Bin	$A_{\hat{T}}(\%)$	$\bar{A}_{\hat{T}}(\%)$	$a_{\hat{P}}^{\hat{T}\text{-odd}}(\%)$	$a_{\hat{CP}}^{\hat{T}\text{-odd}}(\%)$
1	$12.8 \pm 5.4 \pm 1.3$	$2.0 \pm 5.3 \pm 1.3$	$7.4 \pm 3.8 \pm 0.9$	$5.4 \pm 3.8 \pm 0.9$
2	$-9.5 \pm 5.0 \pm 1.2$	$-12.3 \pm 5.0 \pm 1.2$	$-10.9 \pm 3.5 \pm 0.9$	$1.4 \pm 3.5 \pm 0.9$
3	$-5.6 \pm 4.8 \pm 1.2$	$-8.6 \pm 4.8 \pm 1.2$	$-7.1 \pm 3.4 \pm 0.8$	$1.5 \pm 3.4 \pm 0.8$
4	$4.7 \pm 4.8 \pm 1.1$	$-17.7 \pm 4.8 \pm 1.1$	$-6.5 \pm 3.4 \pm 0.8$	$11.2 \pm 3.4 \pm 0.8$
5	$-10.4 \pm 4.8 \pm 1.1$	$-0.3 \pm 4.5 \pm 1.1$	$-5.3 \pm 3.3 \pm 0.8$	$-5.0 \pm 3.3 \pm 0.8$
6	$-14.2 \pm 4.3 \pm 1.1$	$1.0 \pm 4.4 \pm 1.1$	$-6.6 \pm 3.1 \pm 0.8$	$-7.6 \pm 3.1 \pm 0.8$
7	$-5.4 \pm 3.9 \pm 1.2$	$3.8 \pm 3.9 \pm 1.2$	$-0.8 \pm 2.8 \pm 0.8$	$-4.6 \pm 2.8 \pm 0.8$
8	$4.3 \pm 3.8 \pm 1.1$	$-2.3 \pm 3.6 \pm 1.1$	$1.0 \pm 2.6 \pm 0.8$	$3.3 \pm 2.6 \pm 0.8$
9	$3.7 \pm 3.3 \pm 1.0$	$-0.9 \pm 3.3 \pm 1.0$	$1.4 \pm 2.4 \pm 0.7$	$2.3 \pm 2.4 \pm 0.7$
10	$-3.5 \pm 3.3 \pm 1.0$	$0.9 \pm 3.2 \pm 1.0$	$-1.3 \pm 2.3 \pm 0.7$	$-2.2 \pm 2.3 \pm 0.7$

## <sup>10</sup> **References**

- <sup>11</sup> [1] M. Williams, *Observing CP violation in many-body decays*, Phys. Rev. **D84** (2011)  
<sup>12</sup> 054015, [arXiv:1105.5338](#).